Molecular Crystals and Liquid Crystals
Publication details, including instructions for authors and subscription information:
http://www.tandfonline.com/loi/gmcl20

Strong Cubic Optical Nonlinearity of Gold Nanoparticles Suspension in Nematic Liquid Crystal

E. Ouskova [a], D. Lysenko [a], S. Ksondzyk [a], L. Cseh [b], G. H. Mehl [b], V. Reshetnyak [c] & Yu. Reznikov [a]

[a] Institute of Physics, National Academy of Sciences of Ukraine, Kyiv, Ukraine

[b] Department of Chemistry, University of Hull, United Kingdom

[c] National Taras Shevchenko University of Kyiv, Kyiv, Ukraine

Version of record first published: 30 Jun 2011

To cite this article: E. Ouskova, D. Lysenko, S. Ksondzyk, L. Cseh, G. H. Mehl, V. Reshetnyak & Yu. Reznikov (2011): Strong Cubic Optical Nonlinearity of Gold Nanoparticles Suspension in Nematic Liquid Crystal, Molecular Crystals and Liquid Crystals, 545:1, 123/[1347]-132/[1356]

To link to this article: http://dx.doi.org/10.1080/15421406.2011.568883

Mol. Cryst. Liq. Cryst., Vol. 545: pp. 123/[1347]–132/[1356], 2011

ISSN: 1542-1406 print/1563-5287 online
DOI: 10.1080/15421406.2011.568883

Taylor & Francis
Taylor & Francis Group

Strong Cubic Optical Nonlinearity of Gold Nanoparticles Suspension in Nematic Liquid Crystal

E. OUSKOVA,[1] D. LYSENKO,[1] S. KSONDZYK,[1] L. CSEH,[2] G. H. MEHL,[2] V. RESHETNYAK,[3] AND YU. REZNIKOV[1]

[1]Institute of Physics, National Academy of Sciences of Ukraine, Kyiv, Ukraine
[2]Department of Chemistry, University of Hull, United Kingdom
[3]National Taras Shevchenko University of Kyiv, Kyiv, Ukraine

We report on the observations of extremely strong and fast cubic optical nonlinearity in the suspension of gold nanoparticles in nematic liquid crystal (LC). The nonlinearity was observed by recording dynamic phase sinusoidal holograms with a continuous operating laser. It is caused by changes of the refractive index of a LC due to efficient light-induced heating of the nanoparticles at plasmon resonance excitation and following thermal transport of heat to LC matrix. Large nonlinearity parameter ($n_2 \sim 10^{-2}$ cm^2/kW) and fast characteristic times, together with excellent photo- and thermo-stability of the system make its extremely promising for optical processing applications.

Keywords Cubic nonlinearity; gold nanoparticles; holographic gratings; liquid crystal; plasmon resonance

1. Introduction

Suspensions of nanoparticles (NPs) of different nature in liquid crystals (LCs) are of high interest due to a great science and promising applications. LC nano-suspensions give unique opportunity of modifying and controlling of LC properties by non-chemical way and design of novel smart materials. One of the potential applications of LC nano-suspensions is their use as highly nonlinear optical materials for optoelectronics, various nonlinear optical devices, optical switching, beam coupling, etc. [1]. In particular, embedding of absorbing nanoparicles to a LC matrix results in a strong thermal third-order nonlinearity, which is responsible for the variation of refractive index changes of the media [2]. Each particle "works" as effective nano-heater of a LC matrix causing decrease of the order parameter around the particles. As a result, average order parameter of the LC is lowered and, as a

Address correspondence to E. Ouskova, Institute of Physics, National Academy of Sciences of Ukraine, Pr. Nauki 46, Kiev 03028, Ukraine. Tel.: +380-44 525 0779; Fax: +380-44 525 0830; E-mail: ouskova@iop.kiev.ua

consequence, the birefringence of the LC decreases proportional to the light intensity, $\Delta n_a \sim I$. Here we report on the strong thermal cubic nonlinearity of a suspension of gold nanoparticles in nematic LCs in the vicinity of a plasmon resonance band of the particles. A large nonlinearity parameter ($n_2 \sim 10^{-2}\,\mathrm{cm}^2/\mathrm{kW}$) and short characteristic times ($t \sim 1$ ms), together with low aggregation of the particles and excellent photo- and thermo-stability are the distinctive features of the suspension.

2. Materials and Experiments

For preparation of liquid crystal suspension with gold nanoparticles we used commercially available LC E7 and the gold NPs synthesized with the method described by Cseh *et al.* in [3]. First, the gold particles were synthesized which were covered with a hydrocarbon monolayer (hexylthiol chains), and in a second step the surface was functionalized further. The hexylthiol covered gold nanoparticles were reacted with the appropriate mesogen in dichloromethane at ambient temperature for three days to form the monolayer protected LC gold nanoparticles in an exchange reaction. The average particle size was 1.6 ± 0.4 nm, as determined by TEM experiments. The number of gold atoms per particle was approximately 140. The particle surface was covered with hexylthiol and mesogen, and the number of surface-attached chains was approx. 57 ± 5 for the mesogens. A detailed experimental description of the particle synthesis and an analysis of the composition of the structure has already been published in [3]. The schematic structure of gold NP is presented in Figure 1. The combination of liquid crystalline groups and aliphatic chains ensure the easy formation of a liquid crystalline phase behaviour of the particles, as materials consisting of only mesogens attached to gold NPs were found not to exhibit nematic LC behaviour [3 and refs therein]. The alkyl chains act as plastifiers and lower glass transition temperatures and melting points. This effect has also been observed for side-chain polymers and dendrimers and the design principle used for nanoparticles has been discussed in [4].

To prepare the suspension, the gold nanoparticles were dissolved in chloroform and dispersed by a mechanical mixing during 20 min. Then nanoparticles were introduced into LC E7 and chloroform was evaporated at 70°C during one day at constant mechanical stirring. The resulting suspension had a particles concentration, $c_{part} = 1\%$ by weight. A clearing temperature of the suspension, $T_{c,susp} \approx 54.9$°C,

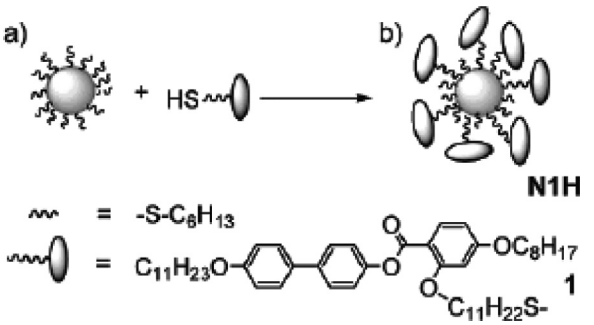

Figure 1. Schematic representations: (a) nanoparticles and (b) exchange reaction. At the bottom: chemical structure of the groups covering the particle (hexylthiol and mesogen) [3].

was lower than the clearing temperature of pure E7, $T_{c,E7} \approx 55.6°C$. This result points towards a little disordering effect of the LC matrix by the gold nanoparticles in the shells.

The suspensions were studied in the planar symmetric cells of the thickness $L = 55\,\mu m$. The inner surfaces of the cell substrates were covered with a polyimide film of poly(4,4′-oxydiphenylene-pyromellitimide) [5]. This material (analogue of a polyimide Capton from DuPont) provided a strong planar anchoring of E7 on the substrates with a low pretilt angle $\theta < 1.5°$. The cells were filled with suspension or pure LC at the temperature above the clearing point (70°C) and cooled down to the room temperature. The suspension in the cell had a light brown colour with a slight gradient of the brightness in the direction of the filling. Several micron-size aggregates were observed in the viewing field of the optical microscope. Observations in the polarisation microscope showed a homogeneous planar texture in the cells. Thus, we can consider that the most of the particles are in the LC either as single particles or as aggregates which size is so small that they cannot distort the director. The director distortion is negligible when the anchoring parameter $\xi = Wl/K << 1$ (W is the anchoring energy, K is the elastic constant, l is the characteristic size of the object). For typical numbers $K = 10^{-7}$ dyne, $W = 10^{-2}\,erg\,cm^{-2}$ $\xi = 1$ at $l = 100\,nm$. So, if some aggregates are in the LC, their size is much smaller than 100 nm. The slight gradient of the optical density in the direction of filling points on a week gradual change of the concentration of the particles or/and aggregates size in the filling direction caused by the LC flow [6].

The suspension was stable during the experiments (at least couple of months). The pretilt angle of the suspension did not differ from the one of the pure LC E7.

The absorption spectrum of the gold nanoparticles in the LC cell is presented in Figure 2. The absorption around 540 nm corresponds to the surface plasmon resonance absorption of the nanoparticles. Despite spherical shapes of the particles and the shell, the spectrum shows an adsorption dichroism, $D_{II}/D_{\perp} \approx 1.1$, and the splitting of the plasmon resonance bands ($\Delta\lambda \approx 10\,nm$) for polarisations parallel (*e*-wave) and perpendicular (*o*-wave) to the director of the LC. This anisotropy is caused by the birefringence of the LC matrix, since both plasmon frequency and plasmon absorption depend on the difference between the refractive indexes of the LC matrix, n_e, n_o, and the effective refractive index of the particles in the shell, $\bar{n}_{part}$ [7].

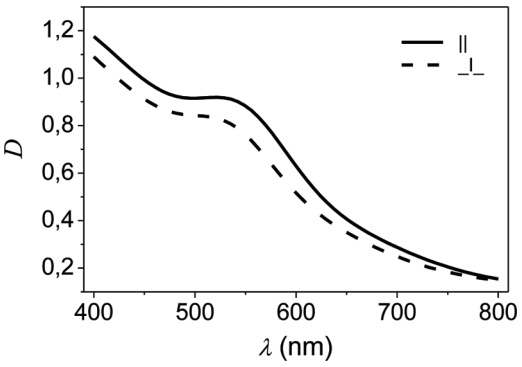

Figure 2. Spectrum of optical density D of gold NPs in LC suspension ($c_{part} = 1\,wt\%$, $L = 55\,\mu m$). Solid line corresponds to *e*-wave (light polarisation is parallel to the director), dash line corresponds to *o*-wave (light polarisation is perpendicular to the director).

The experimental set-up for a dynamic hologram recording is depicted in Figure 3. Two linear polarized Gaussian beams of the equal intensities, $I_{0,pump}/2$, and parallel polarisations, $\vec{E}_{0,pump}$, from the diode-pumped solid state (DPSS) laser "1" ($I_{0,pump} = 0 \div 40\,\mathrm{W/cm^2}$, beam's halfwidth, $w \approx 300\,\mu\mathrm{m}$) intersected in the plane of the LC cell, producing a spatial intensity variation

$$I_{pump} = I_{0,pump} \sin^2(\pi x/\Lambda), \tag{1}$$

where $\Lambda = \lambda_{pump}/2\sin(\phi/2)$ is a period of the interference pattern, $\lambda_{pump} = 532\,\mathrm{nm}$ is a wavelength of the laser irradiation corresponded to the plasmon resonance absorption band of gold nanoparticles. The intensity of the exciting beams and their polarisation $\vec{E}_{0,pump}$ were controlled by neutral filters "2", set of $\lambda/2$-wave plates "3", "7", and polarizer "9". The period of the interference pattern, $\Lambda = 5 \div 50\,\mu\mathrm{m}$, in the plane of the cell was given and controlled by the distance between the parallel beams, d_l, before the lens "8":

$$\Lambda = \frac{\lambda_{pump}}{2\sin(\phi/2)} \approx \frac{F_l}{d_l}\lambda_{pump}.$$

The recording of the holograms was monitored by photodiodes either in the self-diffraction regime by observation of the first order non-Bragg diffraction beams of a DPSS laser behind the LC cell or by observation of the first order diffraction of the probe beam of a He-Ne laser "13". The intensity $I^{(\pm1)}_{d,test}$ and efficiency η_{test} of the test diffraction was connected to a light-induced change of the refractive index of the medium in the maxima of the interference pattern by the formula

$$\eta_{test} = \frac{I^{(\pm1)}_{d,test}}{I_{0,test}} \approx \left(\frac{\pi L}{\lambda_{test}} n_2 I_{0,pump}\right)^2. \tag{2}$$

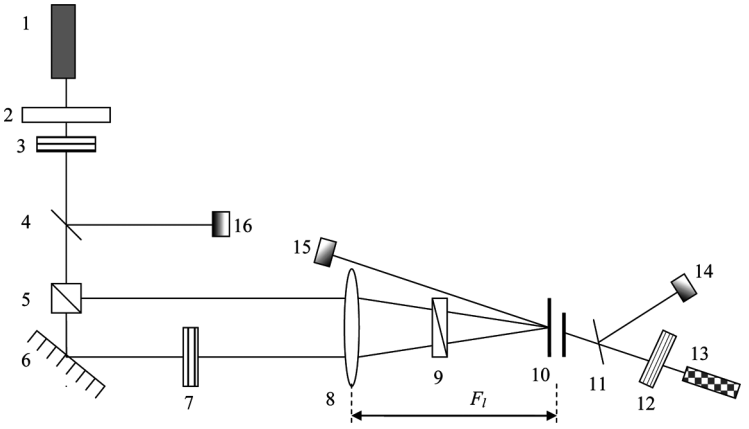

Figure 3. Experimental set-up: 1 – DPSS Laser ($\lambda = 532\,\mathrm{nm}$); 2 – filters; 3, 7, 12 – $\lambda/2$-wave plates; 4, 11 – beam-splitter plates; 5 – beam-splitter cube; 6 – mirrors; 8 – lens; 9 – polarizer; 10 – LC cell; 13 – He-Ne laser ($\lambda = 632.8\,\mathrm{nm}$); 14, 15, 16 – photodiodes.

The polarization of the test beam, $\vec{E}_{0,test}$, and the test diffraction beams, $\vec{E}_{d,test}^{(\pm 1)}$, were given and controlled by the $\lambda/2$-wave plates "12". The director of the suspension, $\vec{d}_{susp}$, was perpendicular the wave vector of the grating, $\vec{q}$. Control of the directions of polarisation vectors, $\vec{E}_{0,pump}$, $\vec{E}_{0,test}$, allowed us to study different configurations of the hologram recording. Below we will denote the configuration of the recording by the indexes *ij*, where the first index corresponds to the polarization (*o*- or *e*-wave) of the both pump beams, and second index denotes the polarization of the test beam (*o*- or *e*-wave).

3. Results

Both self-diffraction and diffraction of the test beam were easily observed in the cells with the suspension but no diffraction was found in the cells with pure LC E7 in all the intensity range of the pump. It shows that the interference pattern in the plane of the cell resulted in the corresponding spatial modulation of the refractive index in the suspension. Besides appearance of the diffraction orders we also observed notable self-defocusing of the beams passed through the cells. This fact indicated a negative sign of the refractive index changes in the suspension, i.e., $\Delta n(I_{pump}) = n_{pump}(I_{pump}) - n_o < 0$.

The dependence of the diffraction efficiency of first order diffraction of the test beam $\eta = \frac{I_{d,test}^{(-1)}}{I_{0,test}} \approx \left(\frac{\pi L}{\lambda_{test}} n_2 I_{0,pump}\right)^2$ [8] *vs* intensity $I_{0,pump}$ for *ee*-configuration is presented in Figure 4. One can see that $\sqrt{\eta}$ linearly increases with $I_{0,pump}$, that is the refractive index of the medium $n(I_{0,pump}) = n + n_2 I_{0,pump}$ (n_2 is nonlinear coefficient), and the medium is described by cubic optical nonlinearity. The linear dependences $\sqrt{\eta(I_{0,pump})}$ were also observed for the other recording configurations.

The linear fitting of the dependence $\sqrt{\eta(I_{0,pump})}$ gives the nonlinear coefficient of refractive index, $n_2^{ee} = 1.9 \times 10^{-2}\,\mathrm{cm}^2/\mathrm{kW}$ that corresponds $n_2^{ee} = 7.8 \times 10^{-3}$ esu. This value is one order bigger than the typical values of n_2 of thermal nonlinearity in absorbing liquid crystals [9].

The diffraction efficiency of the holograms strongly depended on the polarisation of the pump and test beams and their orientation with respect to the wave vector of the grating, $\vec{q}$, $|q| = 2\pi/\Lambda$. By changing the orientation of the vectors

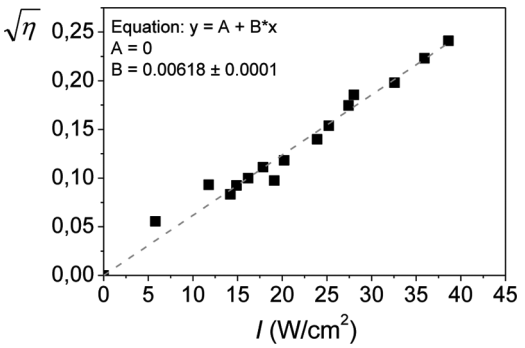

Figure 4. The dependence of $\sqrt{\eta}$ vs. $I_{0,pump}$ for *ee*-configuration, $\Lambda = 50\,\mu\mathrm{m}$. The line represents linear fit; $\sqrt{\eta} = 0.00618 \times I_{0,pump}$.

$\vec{E}_{0,pump}$, $\vec{E}_{0,test}$, and $\vec{d}_{susp}$ we obtained the following relationships between the nonlinear parameters n_2^{ij} for all configurations when diffraction was observed:

$$\frac{n_2^{oe}}{n_2^{ee}} \approx 0.64; \quad \frac{n_2^{eo}}{n_2^{ee}} \approx 10^{-2}; \quad \frac{n_2^{oo}}{n_2^{ee}} \leq 10^{-3}. \tag{3}$$

We did not observe any diffraction at the orthogonal polarizations of the pump beams and there was no diffraction with the change of the polarization of the test beams.

To check if the nonlinearity caused only by gold nanoparticles or anisotropy of LC matrix is important, we recorded the holograms in isotropic phase of the suspension. We found that nonlinearity parameter in the isotropic phase did not depend on the polarization of the pump beams and it was 12 times less than in the nematic phase.

The dependence of diffraction efficiency of dynamic holograms on the grating's period is presented in Figure 5 for *ee*-configuration. This dependence is well described by a function $\eta \sim \Delta n^2 \sim \Lambda^4$, that is the dependence of the refractive index change $\Delta n \propto 1/q^2$. The same type of $\eta(\Lambda)$ dependences was also observed for the other recording configurations.

The dynamics of the grating recording and relaxation were studied by tracking the intensity of the diffraction of the test beam after sharp (<1 ms long) switch-off and switch-on of a one of the recording beams (Fig. 6). The hologram recording, $I_{d,\ test}(t)$ is described by two characteristic times, one of which is fast ($\tau_{fast} \approx 0.7$ ms for $\Lambda = 50\,\mu m$) and the other is rather slow ($\tau_{slow} \approx 1$ s for $\Lambda = 50\,\mu m$). We did not find a change of τ_{slow} with a change of Λ. The time resolution of the experiment did not allowed us to get a numerical values of the dependence $\tau_{fast}(\Lambda)$.

4. Discussion

There are three basic mechanisms of the cubic optical nonlinearity of nematic LCs, which can be observed at irradiation of a LC with a weak-intensity, continuously operating lasers: giant orientational nonlinearity [8], giant conformation nonlinearity [10] and thermal nonlinearity [9]. Orientational nonlinearity can be withdrawn out of the consideration because in the geometry of our experiments (director $\vec{d}_{susp}$ either parallel or perpendicular to the polarization $\vec{E}_{pump}$) the orientation nonlinearity is

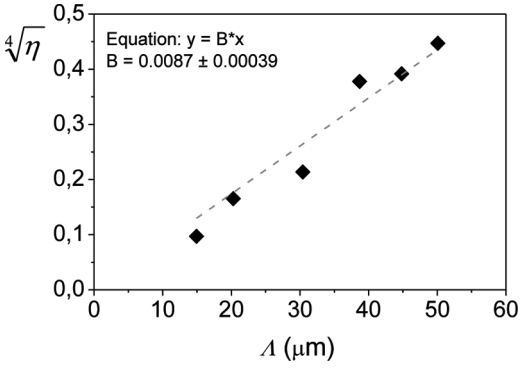

Figure 5. The dependence $\sqrt[4]{\eta(\Lambda)}$ for *ee*-configuration. $I_{0,pump} = 33.5\,W/cm^2$.

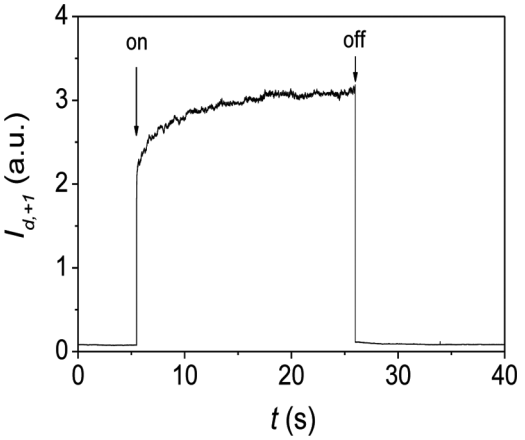

Figure 6. Dynamics of formation and relaxation of gratings. $\Lambda = 50\,\mu m$, $I_{0,pump} = 33.5\,W/cm^2$.

not observed. Moreover, the orientational nonlinearity is a "field-effect" and does not require a light absorption that is not our case. The conformational nonlinearity also can not be responsible for the observed nonlinearity because of strong photo-stability of the gold nanoparticles and their shells. Therefore, we can suggest that a light-induced heating of the particles causes the change of the refractive indexes of the LC due to decrease of the order parameter around the particles.

To check a soundness of this suggestion, let us estimate a heat of LC matrix due to the gold nanoparticles.

The temperature distribution around the particle in an infinite LC matrix is given by the expression [11]:

$$\Delta T = \frac{Q}{4\pi k_{LC}} \frac{1}{r}, \tag{4}$$

where $Q = \alpha_{part} I_{pump} / C_{V,part}$ is a light energy adsorbed by the particles per unit of time, C_V is the volume concentration of the particles without the shells, k_{LC} is the thermoconductivity of the LC (here we neglect the LC thermoconductivity anisotropy), α_{part} is the absorption coefficient of the suspension caused by the absorption of the particles, r is the radius-vector counted from the centre of the particle.

In our case an average distance between the particles, l, is about $30 r_{part}$ and one can neglect by possible overlapping of the heated LC areas. Therefore, we average the distribution $\langle \Delta T(r) \rangle$ over the volume of the LC per one particle:

$$\begin{aligned} \langle \Delta T(r) \rangle &= \frac{1}{V_o} \frac{Q}{4\pi k_{LC}} \int_{r_{part}}^{l/2} \frac{4\pi}{r} r^2 dr \approx C_{V,part} \frac{Q}{2k_{LC}} (l/2)^2 \\ &= \alpha_{part} I_{pump} \frac{1}{2k_{LC}} \left(\frac{3}{4\pi C_{V,part}} \right)^{2/3} \end{aligned} \tag{5}$$

For our values $k_{LC} = 0.15\,W\,m^{-1}\,K^{-1}$ [12], intensity in the maxima of the interference pattern, $I_{pump,max} = 80\,W\,cm^{-2}$, $C_v \approx 2 \times 10^{22}\,m^{-3}$, and absorption coefficient

for e-wave $\alpha^{e}_{part} \approx 9 \times 10^{8}\,\mathrm{m}^{-1}$ the formula (5) leads to $\langle \Delta T \rangle \approx 1.3\ ^{\circ}\mathrm{K}$. Taking into account that for LC E7 at room temperature the derivative $\partial n^{e}/\partial T \approx 10^{-3}$ [13], we arrive at the values $\Delta n^{e} = \partial n^{e}/\partial T \langle \Delta T \rangle \approx 1.2 \times 10^{-3}$ and $n_2^{e} \approx 1.15 \times 10^{-2}\,\mathrm{cm}^2/\mathrm{kW}$ that is close to the experimental number $n_2^{ee} = 1.9 \times 10^{-2}\,\mathrm{cm}^2/\mathrm{kW}$.

The above estimations do not take into account the spatial modulation of the absorbed light energy in the cell. To consider this aspect, we need to solve the question concerning the temperature distribution in a LC cell doped with absorbing nanoparticles in a sinusoidal distributed light field. We will assume homogeneous random distribution of the particles of the same size. Since the distance between the particles $l \approx 200\,\mathrm{nm}$ is much less then the period of the spatial light modulation, $\Lambda \approx 50\,\mu\mathrm{m}$ one can average the absorption of the light by the particles over physically small volume and then employ continuous heaters distribution. In this case the problem is reduced to a solution of the thermoconductivity equation

$$k_{LC}\nabla^2(\Delta T) = -\overline{Q}(1 + \cos qx), \tag{6a}$$

with the boundary conditions

$$T(z = L/2) = T(z = -L/2) = T_0. \tag{6b}$$

Here ΔT is light-induced heating of the LC from the initial temperature T_0, $\overline{Q}$ is the absorbed light energy per unit of time averaged over physically small volume; $\overline{Q} = \alpha I_{pump}$, where $\alpha = \frac{D}{L}\ln 10$ is the averaged absorption coefficient, D is the optical density of the suspension.

The solution of (6) is

$$T = \frac{1}{2k_{LC}}\overline{Q}\left(\left(\frac{L}{2}\right)^2 - z^2\right) + \frac{\overline{Q}}{k_{LC}q^2}\left(1 - \frac{\cosh(qz)}{\cosh\left(q\frac{L}{2}\right)}\right)\cos qx \tag{7}$$

and the averaged over the cell thickness light-induced temperature $\Delta\bar{T}_{\max}$ in the maximum of the interference pattern reads:

$$\Delta\bar{T}_{\max} = \frac{\alpha I_{pump}}{k_{LC}q^2}\left(1 - \frac{2\tanh\left(q\frac{L}{2}\right)}{qL}\right), \tag{8}$$

and finally, the amplitude of the modulation of the refractive index reads:

$$\Delta n^{e,o} = \frac{\partial n^{e,o}}{\partial T}\frac{\alpha I_{pump}}{k_{LC}q^2}\left(1 - \frac{2\tanh\left(q\frac{L}{2}\right)}{qL}\right)\cos qx \tag{9}$$

This formula corresponds qualitatively to the observed dependences of the diffraction efficiency $\eta(I_{0,pump})$ and $\eta(\Lambda)$ (see Figs. 4,5). It also correctly describes the polarisation characteristics of the observed nonlinearity. Indeed, due to adsorption dichroism of spherical NPs in anisotropic LC matrix and birefringence of the LC, the refractive index change and nonlinearity parameter should

depend on polarizations of the pump beams ($i;k = o$ or e) and the test beam ($j;l = o$ or e):

$$\frac{n_2^{ij}}{n_2^{kl}} = \frac{\Delta n^{ij}}{\Delta n^{kl}} = \frac{\alpha^i}{\alpha^k}\frac{\partial n^j/\partial T}{\partial n^l/\partial T} \tag{10}$$

Since $\alpha^e > \alpha^o$ and $\partial n^e/\partial T > \partial n^o/\partial T$, the most strong nonlinearity should be observed for *ee*-configuration and the weakest nonlinearity is for *oo*-configuration that coincides with the experimental data.

As concerning the quantitative comparisons, they show some discrepancy between our estimations and experimental results. For our experimental parameters, $\alpha^e = 3.9 \cdot 10^4\,\mathrm{m}^{-1}$, $\alpha^o = 3.5 \cdot 10^4\,\mathrm{m}^{-1}$ (these values were calculated from the absorption spectrum, Fig. 2), $k_{LC} = k_{LC}^{\perp} = 0.15\,\mathrm{W\,m^{-1}\,K^{-1}}$ [12], $L = 55\,\mu\mathrm{m}$, $q = 1.26 \cdot 10^5\,\mathrm{m}^{-1}$ ($\Lambda = 50\,\mu\mathrm{m}$), $I_{pump} = 40\,\mathrm{W\,cm^{-2}}$, $\partial n^e/\partial T = 10^{-3}\,\mathrm{K}^{-1}$, $\partial n^o/\partial T = 2 \cdot 10^{-6}\,\mathrm{K}^{-1}$, one can get $\Delta\bar{T}^e_{\max} = 6.9^\circ\mathrm{C}$, $\Delta\bar{T}^o_{\max} = 6.2^\circ\mathrm{C}$. These values correspond to the refractive index change $\Delta n^e = 7.5 \cdot 10^{-3}$, $\Delta n^o = 1.25 \cdot 10^{-5}$ and the nonlinearity parameter $n_2^{ee} \approx 2 \cdot 10^{-1}\,\mathrm{cm^2/kW}$, which is almost 10 times higher than the experimental number $n_2^{ee} = 1.9 \cdot 10^{-2}\,\mathrm{cm^2/kW}$.

A smaller discrepancy was found for the relationships between n_2^{ij}. Substituting the values $\partial n^e/\partial T \approx 10^{-3}\,\mathrm{K}^{-1}$, $\partial n^o/\partial T \approx 2 \cdot 10^{-6}\,\mathrm{K}^{-1}$ [13] and $\alpha^o/\alpha^e \approx 0.9$ to (10) we arrive at

$$\frac{n_2^{oe}}{n_2^{ee}} = \frac{\alpha^o}{\alpha^e} \approx 0.9; \quad \frac{n_2^{eo}}{n_2^{ee}} = \frac{\partial n^o/\partial T}{\partial n^e/\partial T} \approx 2 \cdot 10^{-3}; \quad \frac{n_2^{oo}}{n_2^{ee}} = \frac{\alpha^o}{\alpha^e}\frac{\partial n^o/\partial T}{\partial n^e/\partial T} \leq 10^{-4}. \tag{11}$$

When these values are compared with that of (3) it can be seen the discrepancy between the estimated values and experimental results is of the factor 1.5 for n_2^{oe}/n_2^{ee} and of the factor of 5 for n_2^{eo}/n_2^{ee}.

The discrepancies between the estimations and the experimental results exceed the experimental errors and require further studies. At the present state of our knowledge we can suggest two main factors that were not taken into account in the estimations.

- *Light scattering.* In our estimations we neglected the light scattering on the NPs and considered the absorption coefficient equal to the extinction coefficient. Taking into account possible scattering decreases the value α and results in weaker nonlinearity. Our estimations show that for the single NP the scattering is negligibly small in comparison with the absorption but it can be essential in case of NP aggregation which was not studied in our work.
- *Thermoconductivity.* Low concentrated suspensions of NPs have been reported to have enhanced thermal conductivities when compared to pure fluids [14,15]. Therefore, one can suggest that thermal conductivity coefficient used in our estimations was underestimated that might result in less values $\Delta\bar{T}^{e,o}_{\max}$.

5. Conclusions

The results of our studies clearly demonstrate a promise of the LC suspensions of metal NPs as materials with strong and fast cubic optical nonlinearity. Analysis of the collected experimental data and numerical estimations allows us to suggest

strongly that the mechanism of the nonlinearity is caused with changes of the refractive index of a LC due to efficient light-induced heating of the nanoparticles and following thermal transport of heat to LC matrix. At the same time, the estimated values of the measured nonlinearity parameters are to be larger than the experimental ones and the discrepancy exceed the experimental errors. Clarification of the causes of this discrepancy requires additional studies.

References

[1] Ganeev, R. A. (2005). Nonlinear refractionnonlinear absorption of various media. *J. Opt. A: Pure Appl. Opt.*, *7*, 717–733.
[2] Fedorenko, D., Iljina, V., Reshetnyak, V., Slussarenko, S., & Reznikov, Yu. (2001). *Mol. Cryst. Liq. Cryst.*, *375*, 411–423.
[3] Cseh, L., & Mehl, G. (2006). *J. Am. Chem. Soc.*, *128*, 13376–13377.
[4] Cseh, L., & Mehl, G. H. (2007). *J. Mater. Chem.*, *17*, 311.
[5] The polyimide was synthesised by Dr. Gerus, Institute of Bioorganic Chemistry and Petrochemistry, Ukraine.
[6] West, J. L., Glushchenko, A., Liao, G., Reznikov, Yu., Andrienko, D., & Allen, M. P. (2002). *Phys. Rev. E*, *66*, 012702.
[7] Parka, S.-Y., & Stroud, D. (2004). *Appl. Phys. Lett.*, *85*(4), 2920–2923.
[8] Zel'dovich, B., & Tabiryan, N. (1985). in Russian. *Uspehi Phys. Nauk*, *147*(4), 633–674.
[9] Khoo, I.-C., Wu, S.-T. (1993). *Optics and Nonlinear Optics of Liquid Crystals*, World Scientific: Singapore, New Jersy, London, Hong Kong.
[10] Odulov, S. G., Reznikov, Yu. A., Soskin, M. S., & Khizhnyak, A. I. (1982). *JETP*, *55*(5), 854–859.
[11] Govorov, A. O., Zhang, W., Skeini, T., Richardson, H., Lee, J., & Kotov, N. A. (2005). *Nanoscale Research Letters*, *1*(1), 84–90.
[12] Ono, H., & Shibata, K. (2000). *J. Phys. D: Appl. Phys.*, *33*, L137–L140.
[13] Brugioni, S., & Meucci, R. (2007). *Infrared Physics & Technology*, *49*, 210–212.
[14] Putnam, S. A. *et al.* (2006). *J. Appl. Phys.*, *99*, 084308.
[15] Patel, H. E.*et al.* (2003). *Appl. Phys. Lett.*, *83*, 2931–2933.